Journal of Applied Electrochemistry **33**: 197–203, 2003.

Development of a novel redox flow battery for electricity storage system

B. FANG*, Y. WEI, T. ARAI, S. IWASA and M. KUMAGAI
Institute of Research & Innovation, 1201, Takada, Kashiwa, Chiba, 277-0861, Japan
*(*author for correspondence, e-mail: fang@iri.or.jp)*

Received 14 March 2002; accepted in revised form 15 October 2002

Key words: electricity storage, membrane, redox flow battery, vanadium, Vycor glass/silica glass

Abstract

A novel cylindrical battery which uses carbon fibres with high specific surface area as electrodes and a porous silica glass with high chemical stability as membrane has been fabricated. The results obtained from electrolysis of 0.5 M $K_3Fe(CN)_6$–0.5 M KCl and of 85 mM V(IV)–1 M H_2SO_4 indicate that the cell possesses excellent electrolytic efficiency. As a redox flow battery (RFB) its performance was investigated by employing all-vanadium sulfate electrolytes. The results of the cyclic voltammetry measurements indicate that at a glassy carbon electrode the electrochemical window for 2 M H_2SO_4 solution could reach 2.0 $\sim$ 2.4 V. Constant current charging–discharging tests indicate that the batteries could deliver a specific energy of 24 Wh L^{-1} at a current density of 55 mA cm^{-2}. The open-circuit cell voltage, after full charging, remained constant at about 1.51 V for over 72 h, while the coulombic efficiency was over 91%, showing that there was negligible self-discharge due to active ions diffusion through the membrane during this period.

1. Introduction

The redox flow battery (RFB) is one kind of advanced rechargeable battery. For a RFB system, one of the most important features is the possibility of an independent scaling of electric energy storage section (external electrolyte tanks) and of the power section (electrochemical cell). Some of the benefits associated with this technology include low cost, long cycle life, deep-discharge capability and clean and efficient generation of electricity (no waste to dispose). RFB technology is now attracting more and more interest in application for electricity storage systems. Recently, much research and development has been concentrated on all-vanadium redox flow batteries for their excellent performance [1, 2]: (i) there is no decrease in capacity because of the cross mixing of positive electrolyte and negative electrolyte, (ii) all-vanadium RFB does not need catalysts for both electrode reactions, and (iii) there is no evolution of hydrogen gas, which needs rebalancing power and equipment. In short, all-vanadium RFB is a promising technology which has become economically viable. All-vanadium redox batteries will provide advantages for stationary applications such as stand-by power units, load leveling, storage units for solar electricity as well as mobile applications in vehicles for recreational, industrial and city transport wherever pollution-free operation is required [3].

For an all-vanadium RFB system one of the main problems is that the strong oxidative activity of certain kind of vanadium ion (V^{5+}) causes the ion exchange membrane to degrade [4]. For this reason a new type of membrane, Vycor glass (porous silica glass) with high stability and very low cost, was employed in this study.

Carbon felt and/or carbon fiber cloth have been used as electrode materials for all-vanadium RFB systems because of their low cost [5, 6]. In this study, carbon fiber with high specific area was selected as electrode material. Carbon fibers were in intensive contact in the novel battery to ensure low volume resistivity. With carbon fiber as electrodes material and porous silica glass as membrane a vertically assembled cylindrical battery of mini-size was constructed and evaluated.

2. Experimental details

Carbon fibers were chosen as the electrode material for their high specific area, low electrical resistivity and broad voltage window in combination with the electrolyte. Porous Vycor glass with a pore size of around 4.5 nm was chosen as membrane material for its excellent chemical stability and low cost. The membrane used in the battery was 100 mm in length, 17.1 mm in outer diameter and 14.4 mm in inner diameter (inner surface area is about 45.2 cm^2). Carbon fibers with 10 μm in diameter were filled inside the cylindrical membrane to serve as negative electrode of the battery (apparent active surface area 45.2 cm^2). Four bundles of carbon fibers, which were 100 mm in length and 7.2 mm

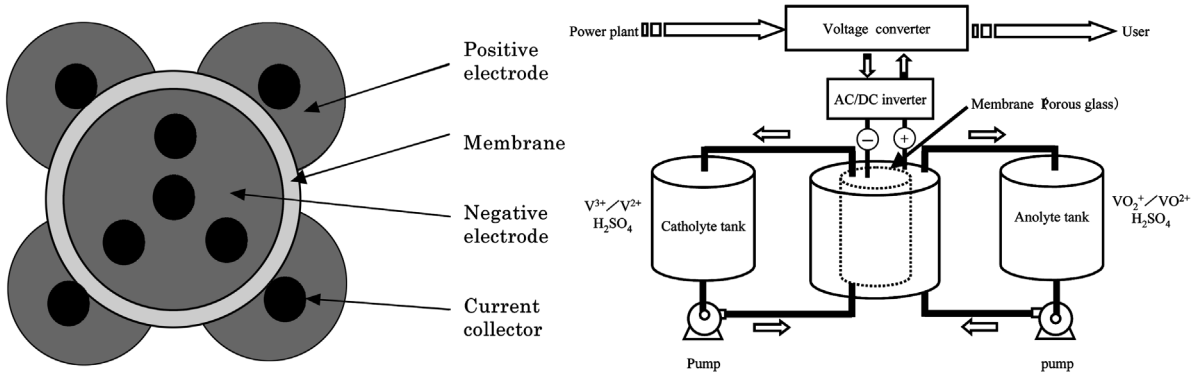

Fig. 1. Schematics of the intersection of the battery (left) and of the RFB system (right).

in bundle diameter each, were arranged evenly around the outside of the membrane as positive electrode of the battery. A graphite rod was inserted into the carbon fibers bundles to serve as the current collector. Schematics of the intersection of the battery (left) and the RFB system (right) are shown in Figure 1.

Microstructures of electrode materials were examined with scanning electron microscopy (SEM) technique.

Pore volume and pore-size distribution in the membrane material, Vycor glass, were examined with BET isothermal adsorption measurement. The area resistivity of Vycor glass and some other membranes were measured using the electrochemical impedance spectrum (EIS) (frequency varied from 100 kHz to 1 Hz) technique. The instruments employed were: model S-5720C frequency response analyser, model HA-501G GP1B potentiostat/galvanostat (Hokuto Denko Corp., Japan). The cell for EIS measurements consisted of two half-cells. A membrane was mounted between the two halves of the cell containing 1 M $VOSO_4$ in 2 M H_2SO_4. Graphite disc and platinum foil electrodes served as working and counter electrodes, respectively. Permeation rates (mass transfer coefficient) of the vanadium species were investigated for a range of membranes by the absorbance measurement [7]. A test membrane (area 7.54 cm^2) was exposed to a solution of 1 M $VOSO_4$ in 2 M H_2SO_4 on one side, and 1 M Na_2SO_4 in 2 M H_2SO_4 on the other side, the Na_2SO_4 being used to equalize the ionic strength of the two solutions and minimize osmotic pressure effects and solvent flow. At regular intervals, a 3 ml sample of the initially vanadium-free solution was withdrawn and its absorbance measured at the appropriate wavelength using a UV-300 visible spectrograph. The sample was then returned to the cell and the procedure continued for up to 30 h. Mass transfer coefficients of $VOSO_4$ for the membranes were calculated from the plot of the absorbance against time.

Electrolytic efficiency of the battery at various flow rates were investigated by potentiostatic electrolysis of 0.5 ml of 0.5 M $K_3Fe(CN)_6$–0.5 M KCl at 100 mV (vs Ag/AgCl). The applied potential for the electrolysis was controlled by a potentiostat/galvanostat (HA-503G, Hokuto Denko Corp.). $K_3Fe(CN)_6$–0.5 M KCl was chosen as the electrolyte to avoid any side reactions (such as hydrogen or oxygen evolution) to occur. Theoretical quantity of the electric charge for the complete electrolysis of 0.5 ml of 0.5 M $K_3Fe(CN)_6$ is calculated as 24.1 C. Practical quantity of the electric charge for the electrolysis was measured by a Coulomb meter (HZ-3000, Hokuto Denko Corp.). The ratio of the practical to theoretical electric-charge was calculated as electrolytic efficiency. Electrolytic efficiency of the battery was also tested by using vanadium ions as electro-active species in sulfuric acid medium, which is commonly used as the electrolyte for redox flow batteries. 100 ml of 85 mM V(IV) in 1 M H_2SO_4 medium was used as the feed solution. Flow rates were varied from 1 to 25 ml min^{-1}. Electrolytic current was kept constant at 50 mA.

A schematic of the test set-up for potentiostatic electrolysis of 0.5 M $K_3Fe(CN)_6$–0.5 M KCl is shown in Figure 2. Prior to injection of 0.5 ml of 0.5 M $K_3Fe(CN)_6$, the deaerated supporting electrolyte (0.5 M KCl) was pumped into both electrode compartments, the test electrode compartment and the counter electrode compartment. A potential of 100 mV vs Ag/AgCl was then applied. When a steady background current was reached, close the valve connected with the inlet of the counter electrode compartment to stop providing the supporting electrolyte. After that, 0.5 ml of 0.5 M $K_3Fe(CN)_6$ solution was injected in pulse and carried into the test electrode compartment by the flowing supporting electrolyte. As a result, the electrolyte in the test electrode compartment was 0.5 M $K_3Fe(CN)_6$–0.5 M KCl and was 0.5 M KCl in the counter electrode compartment.

Half-cell reactions for the battery employing all-vanadium electrolytes were investigated by means of cyclic voltammetry (CV) technique. The electrolyte solutions were deaerated by bubbling with nitrogen both before and during experiments.

Constant-current charge/discharge tests for the redox flow battery were carried out with a battery test system HJ1010SM8 (Hokuto Denko Corp.). The anolyte was 1 M $VOSO_4$ in 2 M H_2SO_4 and catholyte was 1 M $V_2(SO_4)_3$ in 2 M H_2SO_4. Anolyte and catholyte were stored separately in two tanks, and pumped into the positive and negative compartments of the battery during the

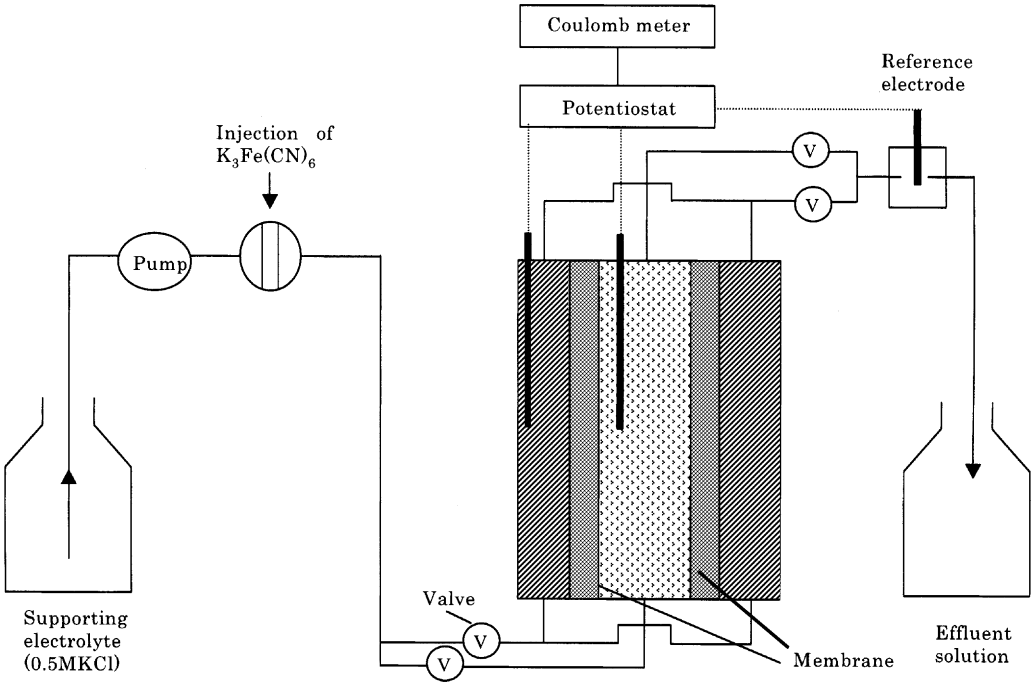

Fig. 2. Sketch of the test set-up for potentiostatic electrolysis of 0.5 M $K_3Fe(CN)_6$–0.5 M KCl.

tests. After full charging, open-circuit voltage was recorded over 72 h while the electrolytes were circulating through the battery.

3. Results and discussion

3.1. *Characterization of electrode and membrane materials*

The SEM photographs of the electrodes material (carbon fibre) are shown in Figure 3. A great number of carbon fibres were bundled together (Figure 3 (a)). Each bundle consisted of approximately 300 carbon fibres. An electrode was composed of many bundles of carbon fibres. From Figure 3 (b) it can be seen that the diameter of each carbon fibre was around 10 μm.

Pore volume and pore-size distribution in the membrane material, Vycor glass, were examined by BET isothermal adsorption measurement. The plot of pore volume against pore diameter calculated from nitrogen adsorption isotherm is shown in Figure 4. It is evident that most pores were around 45 Å in diameter inside the Vycor glass membrane. The differential pore volume in the membrane was about 3.2 ml g^{-1} log^{-1} Å.

Area resistivity of the various membrane materials in 1 M $VOSO_4$–2 M H_2SO_4 solution and mass-transfer coefficients for $VOSO_4$ are listed in Table 1.

Results indicate that the Vycor glass membrane (1.4 mm in thickness) has an area resistivity of 3.3 Ω cm^2, which is a little higher than that of commercial CMV cation exchange membranes (Asahi Glass Co., Japan) often used in the RFBs (~2.0 Ω cm^2) [7], and higher than that of HSV cation exchange membranes recently developed by Sumitomo Electric Industries, Japan (~0.46 Ω cm^2). Results also indicate that Vycor glass membrane in 1.1 mm thickness has relatively low resistivity and permeability. Very small mass-transfer coefficients for the Vycor glass membranes indicate that transfer of vanadium redox species through the Vycor glass membranes were very small.

3.2. *Electrolytic efficiency of the battery at various flow rates*

As shown in Figure 1 (left), since the novel flow type cell contains four partial electrodes as the positive electrode, it is very important for the electrolyte solutions to flow into all the electrodes smoothly at various flow rates to ensure the electroactive species in the solutions can be electrochemically oxidized or reduced effectively during charge and discharge processes. Electrolytic efficiency for the positive and negative electrode at various flow rates are our concern.

Potentiostatic electrolysis of 0.5 ml of 0.5 M $K_3Fe(CN)_6$–0.5 M KCl at 100 mV vs Ag/AgCl at various flow rates were carried out to investigate electrolytic efficiencies of the battery. Electrolysis experiments were repeated three times at each flow rate. The results obtained from the electrolysis at the positive and negative electrodes at various flow rates are shown in Table 2 and Table 3, respectively.

From Table 2 and Table 3, it can be seen that electrolytic efficiencies are almost 100% at the various flow rates for the negative and positive electrodes. This indicates that the electroactive species can be electrochemically oxidized or reduced very effectively at both electrodes of the battery. Constant-current electrolysis

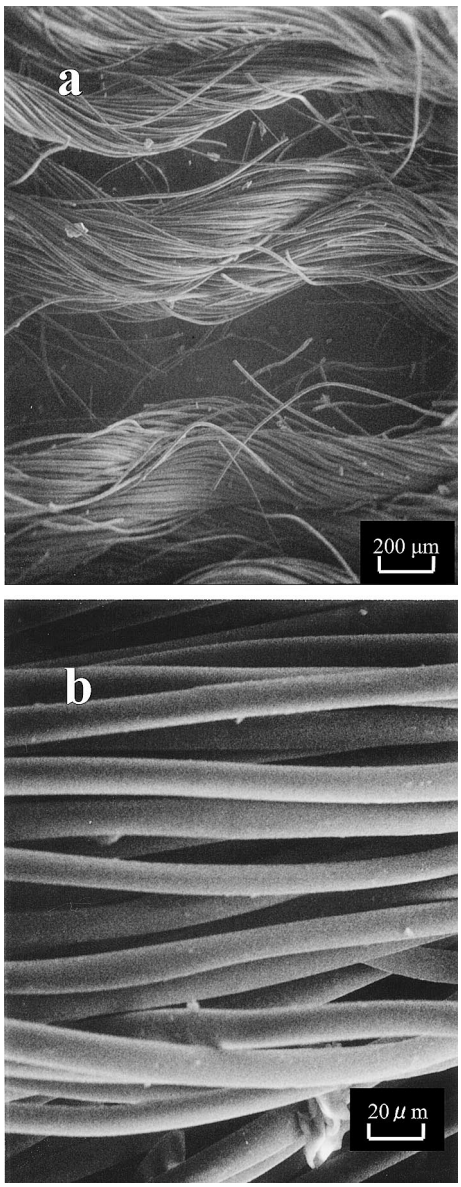

Fig. 3. SEM image of carbon fibres.

of 100 ml of 85 mM $VOSO_4$-1 M H_2SO_4 at various flow rates show that current efficiencies of over 95% were achieved at a deep charge/discharge, which also indicates that the battery possesses excellent electrolytic performance at all applied flow rates.

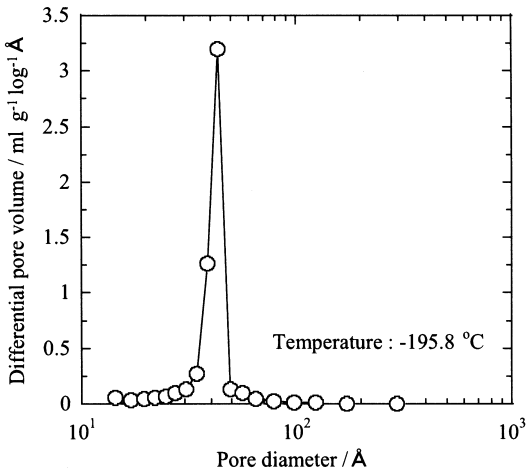

Fig. 4. Pore volume and pore-size distribution in Vycor glass membrane.

Table 1. Area resistivity of the various membranes in 1 M $VOSO_4$–2 M H_2SO_4 and mass-transfer coefficients for $VOSO_4$

Membrane	Area resistivity /Ω cm^2	Mass-transfer coefficients k_s /cm min^{-1}
CMV cation exchange membrane (new)	2.26	5.29×10^{-5}
CMV cation exchange membrane (used)	1.82	5.98×10^{-5}
Vycor glass (1.1 mm in thickness)	2.15	4.61×10^{-5}
Vycor glass (1.4 mm in thickness)	3.31	3.32×10^{-5}
HSV cation exchange membrane	0.46	7.49×10^{-5}

3.3. *Half-cell reactions at the glassy carbon electrode*

Prior to the investigation of electrochemical behaviour of vanadium ions (electro-active species) at glassy carbon electrodes in supporting electrolyte, sulfuric acid, a CV measurement was carried out in 2 M H_2SO_4 without vanadium ions. The result is shown in Figure 5. It is evident that the electrochemical window in 2 M H_2SO_4 solution could reach over 2000 mV, ranging from −400 mV to 1600 mV vs Ag/AgCl.

Electrochemical behaviour of V(IV) species at a glassy carbon electrode in 2 M H_2SO_4 solution is shown in Figure 6.

Table 2. Quantity of the electric charge and electrolytic efficiencies obtained from the negative electrode at various flow rates

Flow rate /ml min^{-1}	Quantity of the electric charge/C				Electrolytic efficiency /%
	1st test	2nd test	3rd test	Average	
1	23.5	24.0	24.2	23.9	99.2
2	23.1	23.9	23.6	23.5	97.6
5	24.8	23.6	24.0	24.1	100.0
10	23.5	25.0	24.2	24.2	100.4
15	24.5	25.0	24.0	24.5	101.7
20	24.8	23.6	24.5	24.3	100.8
25	25.0	24.5	24.0	24.5	101.7

Table 3. Quantity of the electric charge and electrolytic efficiencies obtained from the positive electrode at various flow rates

Flow rate /ml min^{-1}	Quantity of the electric charge/C				Electrolytic efficiency /%
	1st test	2nd test	3rd test	Average	
1	24.0	24.4	25.0	24.5	101.7
2	24.0	25.5	24.5	24.7	102.4
5	23.5	24.5	24.0	24.0	99.6
10	24.5	25.0	24.5	24.7	102.4
15	24.9	23.5	24.5	24.3	100.8
20	24.5	25.5	24.7	24.9	103.3
25	24.0	24.4	24.0	24.1	100.0

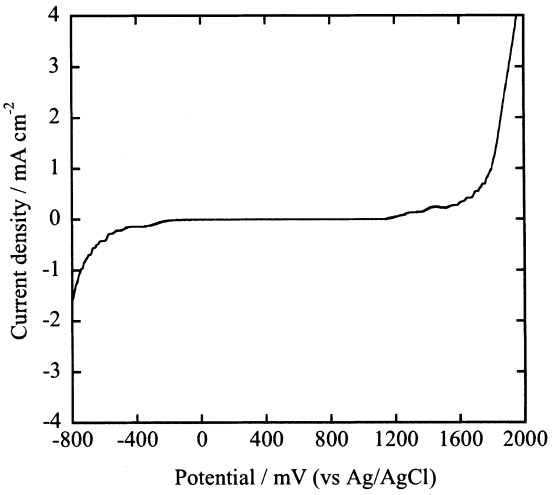

Fig. 5. Cyclic voltammogram obtained at a glassy carbon electrode in 2 M H_2SO_4 solution. Scan rate 100 mV s^{-1}.

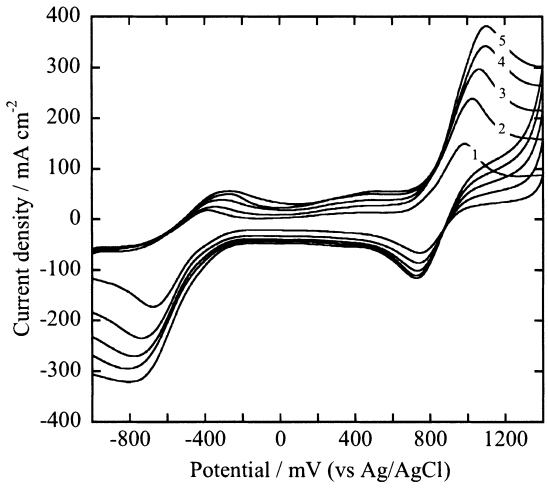

Fig. 6. Cyclic voltammogram obtained at a glassy carbon electrode in 1 M $VOSO_4$–2 M H_2SO_4 solution, Scan rates: (1) 100, (2) 200, (3) 300, (4) 400 and (5) 500 mV s^{-1}.

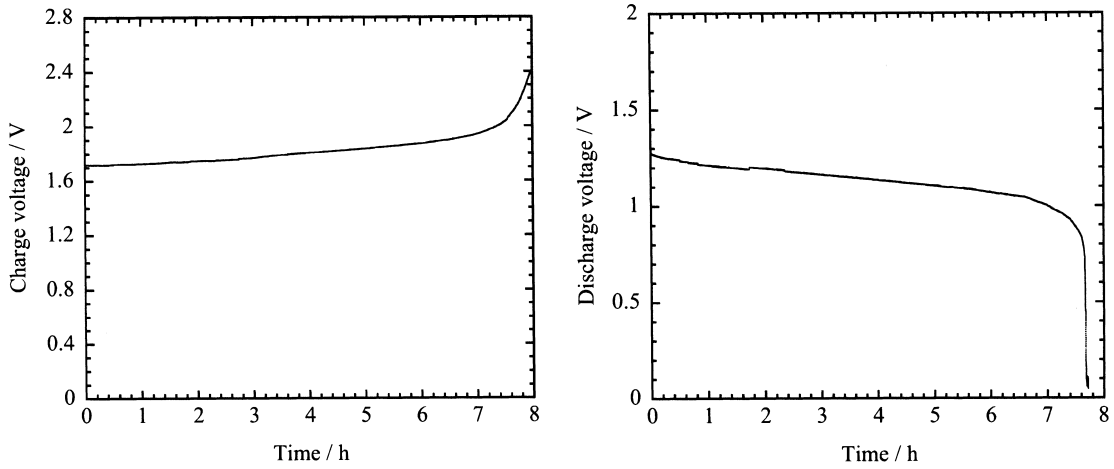

Fig. 7. Typical charge–discharge curve obtained at $I = 2500$ mA (i.e., 55 mA cm^{-2}) for a test cell employing 1 M $VOSO_4$–2 M H_2SO_4 as anolyte and 1 M $V_2(SO_4)_3$–2 M H_2SO_4 as catholyte, $V_{anolyte} = V_{catholyte} = 800$ ml, flow rate: 16.8 ml min^{-1}.

The anodic peak at about 1000 ~ 1100 mV corresponds to the oxidation of V(IV) to V(V) (i.e., $VO^{2+} + H_2O = VO_2^+ + 2H^+ + e^-$), and the corresponding reduction peak occurs at about 700 mV. The anodic peak at about −400 mV and cathodic peak at about −750 mV correspond to the oxidation and reduction of the couple V(II)/V(III), respectively (i.e., $V^{3+} + e^- = V^{2+}$). Because the peak separation between anodic and cathodic peaks was large (it was more than 200 mV even at a low scan rate such as 100 mV s^{-1}, the electron transfer was not very fast for both couples V(IV)/V(V) and V(III)/V(II). The results are in agreement with that reported by Sum et al. [8]. They indicated that V(V)/V(IV) redox couple at glassy-carbon electrodes was electrochemically irreversible and the reversibility of V(III)/V(II) was critically

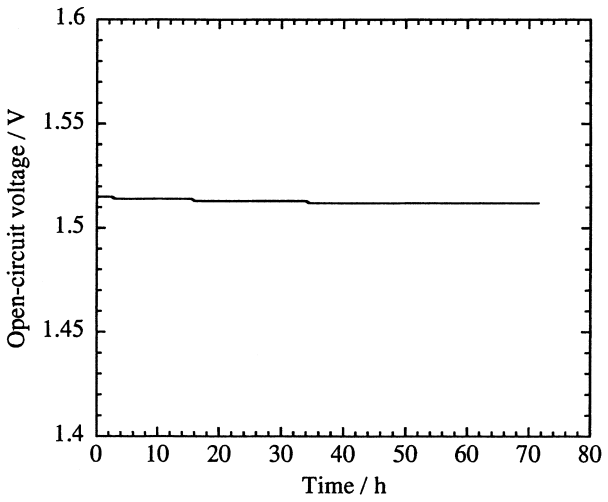

Fig. 8. Plot of open-circuit voltage against time.

dependent upon surface preparation of the glassy-carbon electrode.

3.4. *Charge–discharge performance of the redox flow battery employing all-vanadium electrolytes*

Performance of the novel redox flow battery employing all-vanadium electrolytes was examined by the constant current charge–discharge technique. The electrolyte used for the positive electrode was 1 M $VOSO_4$ in 2 M H_2SO_4 and the volume ($V_{anolyte}$) was 800 ml. The electrolyte used for the negative electrode was 1 M V(III) in 2 M H_2SO_4 and the volume ($V_{catholyte}$) was also 800 ml. Theoretical quantity of the electric charges for complete electrochemical oxidation or reduction of the electroactive species in the electrolyte solutions were calculated to be 77 200 C (21.44 Ah) for both electrodes. The applied current was 2500 mA to charge/discharge the battery for 8 h. The experiment was carried out at 25 °C. Flow rate was 16.8 ml min^{-1}, which is fast enough to ensure even distribution of the electrolyte solution in the four partial positive electrodes and to avoid concentration polarization which may occur at high current density. A typical charge–discharge curve and a plot of open-circuit voltage varying with time are shown in Figures 7 and 8, respectively.

Some data obtained from the charge–discharge test and open-circuit voltage measurement is summarized in Table 4, where Ch. stands for charging and Disch. for discharging.

From Table 4 it was found that the battery could deliver a specific energy of 24 Wh L^{-1} at a current density of 55 mA cm^{-2}. Open-circuit cell voltage after full charging, remained constant at about 1.51 V for over 72 h. The coulombic efficiency of about 97% together with almost constant open-circuit voltage over a long period indicates that there was negligible self-discharge due to cation diffusion through the membrane during this period. On the other hand, voltage efficiency

Table 4. The charging–discharging performance of the battery employing all-vanadium electrolytes ($V_{anolyte} = V_{catholyte} = 800$ ml) at $I = 2500$ mA (i.e., 55 mA cm^{-2})

Flow rate ml min^{-1}	Open-circuit voltage / mV	Average voltage		Quantity of change		Energy		Coulombic efficiency / %	Energy efficiency / %	Voltage efficiency/ %
		Ch. / mV	Disch. / mV	Ch. / Ah	Disch. / Ah	Ch. /Wh	Disch. /Wh			
16.8	1512	1831	1108	19.920	19.296	36.470	21.385	96.9	58.6	60.5

was a little lower, which was a partially attributed to the relatively high membrane resistance. At present, we are examining a new type of membrane of porous silica glass with lower resistivity and permeability. With the new glass membrane further improvement in battery performance is expected.

4. Conclusions

Three conclusions can be drawn: (i) the battery fabricated possesses excellent electrolytic property; (ii) in combination with 2 M H_2SO_4 solution an electrochemical window of about 2.0 $\sim$ 2.4 V was observed at glassy carbon electrodes; and (iii) Open-circuit cell voltage, after full charging, remained constant at about 1.51 V for over 72 h. Coulombic efficiency of about 97% and specific energy of 24 Wh L^{-1} were obtained at a current density of 55 mA cm^{-2}. Self-discharge due to cation diffusion through the membrane during the cycle of charge–discharge and standing period after full charging was negligible.

The novel RFB which uses carbon fibres with high specific surface area as electrodes material and a porous silica glass with high chemical stability as a membrane is promising.

Acknowledgements

This work was financed by NEDO, the New Energy and Industrial Technology Development Organization, Japan. The authors gratefully acknowledge Hokuto Denko Co. for the cooperation in manufacturing the battery.

References

1. M. Skyllas-Kazacos, M. Rychcik, R. Robins, A. Fane and M. Green, *J. Electrochem. Soc.* **133** (1985) 1057.
2. K. Nozaki, H. Kaneko, A. Negishi and T. Ozawa, Japan's Sunshine Project. 1991 Annual Summary of Solar Energy R&D Program. Agency of Industrial Science and Technology, Tokyo (Japan) (1992), p. 481.
3. M. Rychcik and M. Skyllas-Kazacos, *J. Power Sources* **22** (1988) 59.
4. S.C. Chieng, M. Kazacos and M. Skyllas-Kazacos, *J. Power Sources* **39** (1992) 11.
5. H. Kaneko, K. Nozaki, A. Negishi and T. Ozawa, *Electrochimica Acta* **36** (1991) 1191.
6. V. Haddadi-Asl, M. Kazacos and M. Skyllas-Kazacos, *J. Appl. Electrochem.* **25** (1995) 29.
7. F. Grossmith, P. Llewellyn, A.G. Fane and M. Skyllas-Kazacos, Proceedings of the Symposium Stationary Energy Storage: Load Leveling and Remote Applications, Hawaii (1988), p. 363.
8. E. Sum, M. Rychcik and M. Skyllas-Kazacos, *J. Power Sources* **16** (1985) 85.